energies

MDPI

Article

Secure Load Frequency Control of Smart Grids under Deception Attack: A Piecewise Delay Approach

Fei Zhao [1,*], Jinsha Yuan [1], Ning Wang [1], Zhang Zhang [2] and Helong Wen [3]

[1] School of Electrical and Electronic Engineering, North China Electric Power University, Baoding 071003, China; yuanjinsha@ncepu.edu.cn (J.Y.); wangning@ncepu.edu.cn (N.W.)
[2] State Grid Hebei Economic Research Institute, Shijiazhuang 050021, China; zhzh019@163.com
[3] State Grid Handan Fengfeng Kuangqu Power Supply Company, Handan 056200, China; ncepuwen@163.com
* Correspondence: zhaofei@ncepu.edu.cn; Tel.: +86-312-752-2909

Received: 14 May 2019; Accepted: 11 June 2019; Published: 13 June 2019

Abstract: The problem of secure load frequency control of smart grids is investigated in this paper. The networked data transmission within the smart grid is corrupted by stochastic deception attacks. First, a unified Load frequency control model is constructed to account for both network-induced effects and deception attacks. Second, with the Lyapunov functional method, a piecewise delay analysis is conducted to study the stability of the established model, which is of less conservativeness. Third, based on the stability analysis, a controller design method is provided in terms of linear matrix inequalities. Finally, a case study is carried out to demonstrate the derived results.

Keywords: load frequency control; multi-area power systems; network communication; deception attack

1. Introduction

In recent years, the smart grid has become a significant generation of power system network to provide high quality power service for 21st century needs. For the purpose of energy scheduling, overall regulation and the quality of power service, interconnected multi-area power systems are pivotal in the operation of a smart grid [1]. An important objective of a power system is to study the equilibrium problem or stability analysis of frequency, of which the variation mainly depends on the active power. In the 1970s, Elgerd and Fosha firstly applied Control Theory to the load frequency control (LFC) problem of interconnected power systems [2]. Since then, many researchers have been working on the LFC analysis with variety of control methods [3–9]. To mention a few, Reference [3] designed an adaptive load frequency controller for a two-area power system and proposed an optimal control scheme. An optimization approach for LFC controller design with genetic algorithms was presented in [4], where the criteria were given in terms of linear matrix inequalities (LMIs). Reference [5] investigated the LFC problem of isolated grid and proposed a multivariable generalized predictive controller.

On the other hand, networked control systems have been a hot topic in past decades. With wireless communication between devices, the superiority on more flexibility, less cost and convenient maintenance enable this type of system to play a significant role in many fields such as wireless communication, industrial manufacturing and intelligent control. However, in a networked control system, transmission delays and packet dropouts are inevitable in data communication, which would affect or even deteriorate the stability and control performance. Many results on network-based system analyses were carried out in [10–15] taking into account the network-induced delays and packet losses. Note that most of the obtained results are delay-dependent. To reduce the conservativeness of these results, a few novel analysis methods were presented, such as free weighting matrix [16],

the input–output approach [17], and piecewise analysis method [18]. Specifically, the idea of the piecewise analysis method was firstly proposed in [19], where the time delay's variation interval was divided into two subintervals with equal length according to a central point. Reference [18] then extended this method and investigated the stability of both discrete and continuous time systems with more than two subintervals divided. In addition, the conservativeness of the method was also discussed compared with other existing works.

With the popularity of interconnected multi-area power systems, the power system network is becoming more and more complex. Thus, control and regulation of power systems through wireless communication is of significance. In a network communication environment, other than the network-induced phenomena mentioned above, open channels also encounter serious security issues. Some malicious adversaries may launch invasive attacks into data transmission networks in a smart grid, resulting in significant impacts on the national economy and social stability. Thus, the the security issues concerned with power systems should be valued. In existing works, some results on secure performance of power systems have been presented [20–25]. Specifically, references [20,21] were concerned with the load redistribution attacks in power systems and investigated the modeling method and secure estimation problem, respectively. Reference [22] designed a defending method against time delay attacks into LFC mechanism of distributed power systems. An event-triggered scheme was proposed in [23] to compensate the effects of denial-of-service attacks in smart grid. Reference [24] investigated a type of resonance attacks on LFC problem in multiple area power systems. However, there has been little attention paid to secure LFC of smart grids under stochastic deception attacks. Deception attacks [26] can stochastically deteriorate the integrity of a transmitted data packet and severely affect the performance of power systems, which should not be neglected in the secure control of power systems, especial in an interconnected power system network in a smart grid.

In this paper, the secure LFC problem of smart grids is addressed. The data packets received and sent by the remote PI controller encounter, not only network-induced phenomena. but also deception attacks launched by adversaries. The rest of the paper is arranged as follows. In Section 2, a unified model for network-based LFC of multi-area power systems is established taking into account networked phenomena and deception attacks. In Section 3, a piecewise delay method is used to constructed Lyapunv–Krasovskii function, through which the stability of established system model is analyzed. Based on the criteria on stability, the design method for desired PI controller is proposed. In Section 4, a case study of three area power systems is given to show the effectiveness of the obtained results. Finally, a conclusion is stated in Section 5.

Notations: $\mathbb{R}^n$ denotes the n dimensional Euclidean space. $\mathbb{R}^n_+$ denotes the positive orthant of $\mathbb{R}^n$. Augmented matrix $\text{diag}_N\{U\}$ ($\text{diag}_N\{U_i\}$) represents the diagonal matrix $\text{diag}\{U, ..., U\}$ ($\text{diag}\{U_1, ..., U_N\}$) of N blocks. $\mathbb{E}\{\cdot\}$ represents the mathematical expectation. The matrices in the current research are all assumed to have compatible dimensions.

2. Preliminaries

In this section, a unified system model for LFC of a multiple area power system with corrupted network communication will be constructed. In the specific modeling, the adversarial attacks as well as network-induced phenomena including transmission delay, packet loss and packet disorder are all taken into account.

2.1. Multi-Area Power Systems in Smart Grid

The diagram of ith area power system in a smart grid is given in Figure 1, which is similar to that of [23,27]. Based on this diagram of ith area power system, we will elaborate the operation of multiple area power systems with network-based load frequency controller in the following.

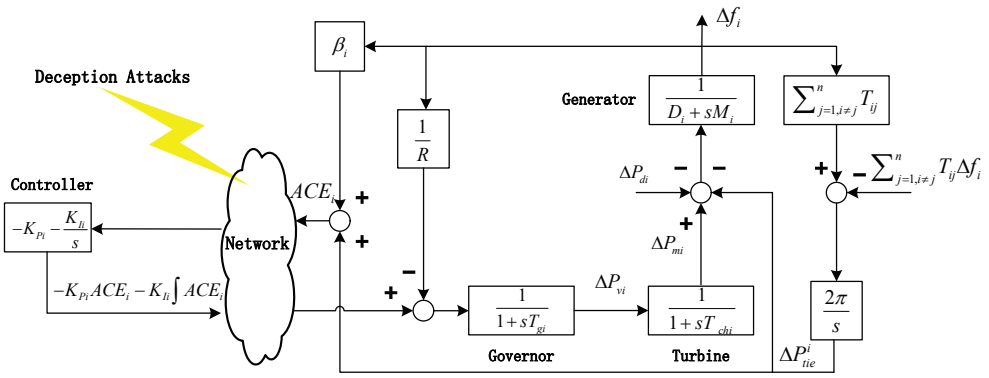

Figure 1. The framework of network-based LFC of *i*th area power system.

The deviation of frequency of *i*-th power system area is given by

$$\Delta \dot{f}_i = -\frac{D_i}{M_i}\Delta f_i - \frac{1}{M_i}\Delta P^i_{tie} + \frac{1}{M_i}\Delta P_{mi} - \frac{1}{M_i}\Delta P_{di} \tag{1}$$

where Δf_i is the frequency deviation in area i; ΔP^i_{tie} denotes the deviation of tie-line power exchange between areas; ΔP_{mi} denotes the mechanical output deviation of generator; ΔP_{di} is the i-th load deviation; D_i is the damping coefficient of area i; M_i denotes the inertia of the generator in area i.

The deviation of tie-line power exchange between two areas is described by

$$\Delta \dot{P}^i_{tie} = 2\pi \sum_{j=1, j\neq i}^{n} T_{ij}(\Delta f_i - \Delta f_j) \tag{2}$$

where T_{ij} is the synchronization coefficient between area i and j.

The valve position equation is governed by

$$\Delta \dot{P}_{vi} = -\frac{1}{R_i T_{gi}}\Delta f_i - \frac{1}{T_{gi}}\Delta P_{vi} + \frac{1}{T_{gi}}u_i(t) \tag{3}$$

where ΔP denotes the deviation of ith valve position; $u_i(t)$ is the control input of area i; R_i is the droop coefficient of area i; T_{gi} denotes the time constant of the governor in ith area.

The mechanical power equation of generator is given as

$$\Delta \dot{P}_{mi} = -\frac{1}{T_{chi}}\Delta P_{mi} + \frac{1}{T_{chi}}\Delta P_{vi} \tag{4}$$

where T_{chi} is the time constant of the turbine. Furthermore, in area i, the ACE signal is defined as

$$ACE_i = \beta_i \Delta f_i + \Delta P^i_{tie} \tag{5}$$

Consisting of frequency deviation and net power exchange, ACE is the input signal of PI controller, of which the control scheme is designed as

$$u_i(t) = -K_{Pi}ACE_i(t) - K_{Ii}\int ACE_i(t) \tag{6}$$

where K_{Pi} and K_{Ii} are the proportional gain and integral gain of the PI controller.

Combining the above analyses, and defining

$$x(t) = [x_1^{\mathrm{T}}(t), x_2^{\mathrm{T}}(t), ..., x_n^{\mathrm{T}}(t)]^{\mathrm{T}},\ u(t) = [u_1^{\mathrm{T}}(t), u_2^{\mathrm{T}}(t), ..., u_n^{\mathrm{T}}(t)]^{\mathrm{T}}$$
$$y(t) = [y_1(t)^{\mathrm{T}}, y_2(t)^{\mathrm{T}}, ..., y_n(t)^{\mathrm{T}}]^{\mathrm{T}},\ w(t) = [\Delta P_{d1}(t), \Delta P_{d2}(t), ..., \Delta P_{dn}(t)]^{\mathrm{T}}$$

$$x_i(t) = [\Delta f_i, \Delta P_{tie}^i, \Delta P_{mi}, \Delta P_{vi}, \int ACE_i]^{\mathrm{T}},\ y_i(t) = [ACE_i(t), \int ACE_i(t)]^{\mathrm{T}}$$
$$A = [A_{ij}]_{n\times n},\ B = \mathrm{diag}_n\{B_i\},\ C = \mathrm{diag}_n\{C_i\},\ F = \mathrm{diag}_n\{F_i\}$$

we can derive an augmented model of multiple area smart grid system as

$$\begin{cases} \dot{x}(t) = Ax(t) + Bu(t) + Fw(t) \\ y(t) = Cx(t) \end{cases} \tag{7}$$

with

$$A_{ii} = \begin{bmatrix} -\frac{D_i}{M_i} & -\frac{1}{M_i} & \frac{1}{M_i} & 0 & 0 \\ 2\pi\sum_{j=1,j\neq i}^{n} T_{ij} & 0 & 0 & 0 & 0 \\ 0 & 0 & -\frac{1}{T_{chi}} & \frac{1}{T_{chi}} & 0 \\ -\frac{1}{R_i T_{gi}} & 0 & 0 & -\frac{1}{T_{gi}} & 0 \\ \beta_i & 1 & 0 & 0 & 0 \end{bmatrix},\ A_{ij} = \begin{bmatrix} 0 & 0 & 0 & 0 & 0 \\ -2\pi T_{ij} & 0 & 0 & 0 & 0 \\ 0 & 0 & 0 & 0 & 0 \\ 0 & 0 & 0 & 0 & 0 \\ 0 & 0 & 0 & 0 & 0 \end{bmatrix}$$

$$B_i = \begin{bmatrix} 0 \\ 0 \\ 0 \\ \frac{1}{T_{gi}} \\ 0 \end{bmatrix}, F_i = \begin{bmatrix} -\frac{1}{M_i} \\ 0 \\ 0 \\ 0 \\ 0 \end{bmatrix}, C_i = \begin{bmatrix} \beta_i & 1 & 0 & 0 & 0 \\ 0 & 0 & 0 & 0 & 1 \end{bmatrix}$$

and we also have the augmented load frequency control signal is

$$u(t) = Ky(t) = KCx(t) \tag{8}$$

where $K = \mathrm{diag}_n\{K_i\}$ and $K_i = [-K_{Pi}, -K_{Ii}]$.

2.2. LFC under Corrupted Network Communication

In the current research, the ACE signal will be transmitted to a PI controller through wireless network channels, which leads to inevitable network-induced phenomena including transmission delays, packet dropouts, packet disorders and so on. Denoted by h the sampling period. $i_k, k = 1, 2, ...$ are integers satisfying $\{i_1, i_2, ...\} \subset \{s | s = 1, 2, ...\}$. Then $sh, s = 1, 2, ...$ denote all the sampling instants. $i_k h$ denotes the sampling instant of the data packet which successfully arrives at the controller side. All the data packets have been stamped with time stamp before transmitted. With the employed ZOH, the data information will not be updated until the ZOH receive a new packet. Another important function of ZOH is to avoid packet disorder. Specifically, if the packet $x((sh), s)$ with stamp s reaches ZOH earlier than packet $(x((s-1)h), s-1)$ due to the network-induced delay or packet loss, the packet with stamp $s-1$ will be ignored and packet $x((sh), s)$ will be updated to the controller side. Thus, with the effects of networked communication, we have

$$u(t) = KCx(i_k h),\ t \in [i_k h + \tau_k, i_{k+1} h + \tau_{k+1}) \tag{9}$$

where τ_k is the network-induced delay denoting the time from the sampling instant $i_k h$ to the instant when the governor receive the control signal. It is noted that if $i_{k+1} = i_k + 1$, then there is no packet dropout between packets $(x(i_k h), i_k)$ and $(x(i_{k+})h, i_{k+1})$; if $i_{k+1} = i_k + p + 1$, $p \in \mathbb{N}_+$, p packets have been dropped during network transmission.

Due to the open broadcasting nature of network communication, the wireless transmission is vulnerable to adversarial attacks. Considering the effects of deception attacks which can deteriorate the integrity of the transmitted signal, we can derive the corrupted control signal $\tilde{u}$ as

$$\tilde{u}(t) = u(t) + \alpha(t)v(t) \tag{10}$$

where $v(t) = -u(t) + \xi(t)$ is the deception attack signal launched by adversaries and $\xi(t)$ is an energy-bounded signal belonging to $\mathcal{L}_2[0, +\infty)$. $\alpha(t)$ is a stochastic variable subject to Bernoulli distribution with probabilities $\text{Prob}\{\alpha(t) = 1\} = \alpha_0$ and $\text{Prob}\{\alpha(t) = 0\} = 1 - \alpha_0$, $\alpha_0 \in [0, 1)$.

Furthermore, we let $\tau(t) = t - i_k h$, $t \in [i_k h + \tau_k, i_{k+1} h + \tau_{k+1})$. It is easy to have

$$\tau_m \leq \tau_k \leq \tau(t) \leq i_{k+1} h - i_k h + \tau_{k+1} \leq \tau_M$$

where τ_m and τ_M are two known constants.

Thus, the networked control signal can be written as

$$u(t) = (1 - \alpha(t))KCx(t - \tau(t)) + \alpha(t)\xi(t),\ t \in [i_k h + \tau_k, i_{k+1} h + \tau_{k+1}) \tag{11}$$

based on which, (7) should be expressed as

$$\begin{cases} \dot{x}(t) = Ax(t) + (1 - \alpha(t))BKCx(t - \tau(t)) + \alpha(t)B\xi(t) + Fw(t) \\ y(t) = Cx(t),\ t \in [i_k h + \tau_k, i_{k+1} h + \tau_{k+1}) \end{cases} \tag{12}$$

Remark 1. *Combining the above analyses, construction of system (12) synthesizing the network-induced time delay, packet dropout, packet disorder and deception attack. Specifically, time interval $[i_k h + \tau_k, i_{k+1} h + \tau_{k+1})$ describes the varying transmission delays and packet dropouts. ZOHs prevent the negative effects of packet disorders. Through defining the stochastic variable $\alpha(t)$, the deception attacks can be easily processed into parameters of system model.*

To facilitate the LFC analysis of multiple area power systems, the following two Lemmas need to be introduced.

Lemma 1. *[28] Under the condition $\bar{\tau}_m \leq \tau(t) \leq \bar{\tau}_M$ and $\dot{x}(t + \cdot) : [-\bar{\tau}_M, -\bar{\tau}_m] \to \mathbb{R}^n$, $t \in \mathbb{R}_+$, then the following inequality holds for $\forall R > 0$:*

$$-(\bar{\tau}_M - \bar{\tau}_m) \int_{t-\bar{\tau}_M}^{t-\bar{\tau}_m} \dot{x}^{\mathrm{T}}(s) R \dot{x}(s) \mathrm{d}s \leq \begin{bmatrix} x(t - \bar{\tau}_m) \\ x(t - \bar{\tau}_M) \end{bmatrix}^{\mathrm{T}} \begin{bmatrix} -R & R \\ R & -R \end{bmatrix} \begin{bmatrix} x(t - \bar{\tau}_m) \\ x(t - \bar{\tau}_M) \end{bmatrix} \tag{13}$$

Lemma 2. *[29] For $\forall x, y \in \mathbb{R}^n$, and a positive scalar ϵ, one have*

$$x^{\mathrm{T}} y + y^{\mathrm{T}} x \leq \epsilon x^{\mathrm{T}} x + \epsilon^{-1} y^{\mathrm{T}} y \tag{14}$$

Lemma 3. *[18] Under the condition $\bar{\tau}_m \leq \tau(t) \leq \bar{\tau}_M$ where $\tau(\cdot) : \mathbb{R}_+ \to \mathbb{R}_+$, for any constant matrices Ξ_1, Ξ_2 and Ω, inequality*

$$(\tau(t) - \bar{\tau}_m)\Xi_1 + (\bar{\tau}_M - \tau(t))\Xi_2 + \Omega < 0$$

holds if and only if

$$(\bar{\tau}_M - \bar{\tau}_m)\Xi_1 + \Omega < 0$$
$$(\bar{\tau}_M - \bar{\tau}_m)\Xi_2 + \Omega < 0$$

The objective of this paper is to design a PI controller for multiple area power systems such that

(1) System (12) with both $w(t) = 0$ and $\xi(t) = 0$ is asymptotically stable;
(2) For nonzero load signal $w(t)$ and attack signal $\xi(t)$, system (12) under zero initial condition is said to satisfy H_∞ performance if the following inequality holds:

$$\mathbb{E}\{\|y(t)\|_2\} \leq \gamma \mathbb{E}\{\|w(t)\|_2 + \|\xi(t)\|_2\}$$

3. Main Results

In this section, through a piecewise delay method, the sufficient conditions for H_∞ stability of system (12) are proposed. Then, with some reasonable matrix processing, a design approach to controller gain is provided with the presence of deception attacks.

To facilitate the following development, (12) can be further written as

$$\dot{x}(t) = \phi(t) + (\alpha_0 - \alpha(t))\psi(t) \tag{15}$$

where

$$\begin{aligned}\phi(t) &= Ax(t) + (1-\alpha_0)BKCx(t-\tau(t)) + \alpha_0 B\xi(t) + Fw(t)\\ \psi(t) &= BKCx(t-\tau(t)) - B\xi(t)\end{aligned}$$

To reduce the conservativeness of the analysis, the variation range of delay $\tau(t)$ is divided into two intervals with equal length. Let $\delta = \frac{\tau_M - \tau_m}{2}$ and $\tau_0 = \tau_m + \delta$, then two sets can be defined as

$$\begin{aligned}\Theta_1 &= \{t|\tau(t) \in [\tau_m, \tau_0]\}\\ \Theta_2 &= \{t|\tau(t) \in [\tau_0, \tau_M]\}\end{aligned}$$

from which one can have $\Theta_1 \bigcup \Theta_2 = \mathbb{R}^+$ and $\Theta_1 \bigcap \Theta_2 = \emptyset$. In the sequent research, we mainly investigate the performance of system (15) over these two sets.

3.1. H_∞ Stability Analysis

Theorem 1. *For given scalars $\alpha_0 \geq 0$, $\gamma > 0$, $\tau_M \geq \tau_m \geq 0$ and matrices K, system (12) is asymptotically stable satisfying H_∞ performance if there exist positive definite matrices R_1, R_2, R_3, M, N, S and T such that the following inequalities hold:*

$$\begin{bmatrix}\Phi_i + \Sigma_{11}^i + (\Sigma_{11}^i)^{\mathrm{T}} & * & *\\ \Sigma_{21}^{ij} & \Sigma_{22}^i & *\\ \Sigma_{31} & 0 & \Sigma_{33}\end{bmatrix} < 0,\ i = 1,2\ j = 1,2 \tag{16}$$

where

$$\Phi_1 = \begin{bmatrix}\Phi_{11} & * & * & * & * & * & *\\ (1-\alpha_0)C^{\mathrm{T}}K^{\mathrm{T}}B^{\mathrm{T}}P & 0 & * & * & * & * & *\\ R_1 & 0 & -Q_1 - R_1 & * & * & * & *\\ 0 & 0 & 0 & -Q_2 - \frac{R_3}{\delta} & * & * & *\\ 0 & 0 & 0 & \frac{R_3}{\delta} & -Q_3 - \frac{R_3}{\delta} & * & *\\ F^{\mathrm{T}}P & 0 & 0 & 0 & 0 & -\gamma^2 I & *\\ \alpha_0 B^{\mathrm{T}}P & 0 & 0 & 0 & 0 & 0 & -\gamma^2 I\end{bmatrix}$$

$$\Phi_{11} = PA + A^{\mathrm{T}}P + Q_1 + Q_2 + Q_3 - R_1 + C^{\mathrm{T}}C$$

$$\Phi_2 = \begin{bmatrix} \Phi_{11} & * & * & * & * & * & * \\ (1-\alpha_0)C^{\mathrm{T}}K^{\mathrm{T}}B^{\mathrm{T}}P & 0 & * & * & * & * & * \\ R_1 & 0 & -Q_1 - R_1 - \frac{R_2}{\delta} & * & * & * & * \\ 0 & 0 & \frac{R_2}{\delta} & -Q_2 - \frac{R_2}{\delta} & * & * & * \\ 0 & 0 & 0 & 0 & -Q_3 & * & * \\ F^{\mathrm{T}}P & 0 & 0 & 0 & 0 & -\gamma^2 I & * \\ \alpha_0 C^{\mathrm{T}}B^{\mathrm{T}}P & 0 & 0 & 0 & 0 & 0 & -\gamma^2 I \end{bmatrix}$$

$$\Sigma_{11}^1 = \begin{bmatrix} 0 & -N+M & N & -M & 0 & 0 & 0 \end{bmatrix}$$

$$\Sigma_{11}^2 = \begin{bmatrix} 0 & T-S & 0 & S & -T & 0 & 0 \end{bmatrix}$$

$$\Sigma_{21}^{11} = \sqrt{\delta}N^{\mathrm{T}},\ \Sigma_{21}^{12} = \sqrt{\delta}M^{\mathrm{T}},\ \Sigma_{21}^{21} = \sqrt{\delta}S^{\mathrm{T}},\ \Sigma_{21}^{22} = \sqrt{\delta}T^{\mathrm{T}}$$

$$\Sigma_{22}^1 = -R_2,\ \Sigma_{22}^2 = -R_3$$

$$\Sigma_{31} = \begin{bmatrix} \tau_m R_1 \mathcal{A}_\phi \\ \sqrt{\delta} R_2 \mathcal{A}_\phi \\ \sqrt{\delta} R_3 \mathcal{A}_\phi \\ \tau_m \sqrt{\alpha_0(1-\alpha_0)\delta} R_1 \mathcal{A}_\psi \\ \sqrt{\alpha_0(1-\alpha_0)\delta} R_2 \mathcal{A}_\psi \\ \sqrt{\alpha_0(1-\alpha_0)\delta} R_3 \mathcal{A}_\psi \end{bmatrix},\ \Sigma_{33} = \mathrm{diag}\{-R_1, -R_2, -R_3, -R_1, -R_2, -R_3\}$$

$$\mathcal{A}_\phi = \begin{bmatrix} A & BKC & 0 & 0 & 0 & F & \alpha_0 B \end{bmatrix}$$

$$\mathcal{A}_\psi = \begin{bmatrix} 0 & BKC & 0 & 0 & 0 & 0 & -B \end{bmatrix}$$

Proof of Theorem 1. A Lyapunov-Krasovskii functional $V(x(t))$ is built as

$$V(x(t)) = V_1(x(t)) + V_2(x(t)) + V_3(x(t)) \tag{17}$$

where

$$\begin{aligned} V_1(x(t)) &= x^{\mathrm{T}}(t)Px(t) \\ V_2(x(t)) &= \int_{t-\tau_m}^{t} x^{\mathrm{T}}(s)Q_1x(s)\mathrm{d}s + \int_{t-\tau_0}^{t} x^{\mathrm{T}}(s)Q_2x(s)\mathrm{d}s + \int_{t-\tau_M}^{t} x^{\mathrm{T}}(s)Q_3x(s)\mathrm{d}s \\ V_3(x(t)) &= \tau_m \int_{t-\tau_m}^{t}\int_{s}^{t} \dot{x}^{\mathrm{T}}(v)R_1\dot{x}(v)\mathrm{d}v\mathrm{d}s + \int_{t-\tau_0}^{t-\tau_m}\int_{s}^{t} \dot{x}^{\mathrm{T}}(v)R_2\dot{x}(v)\mathrm{d}v\mathrm{d}s \\ &\quad + \int_{t-\tau_M}^{t-\tau_0}\int_{s}^{t} \dot{x}^{\mathrm{T}}(v)R_3\dot{x}(v)\mathrm{d}v\mathrm{d}s \end{aligned}$$

Calculating the expectation of derivative $\mathcal{L}V(x(t))$, we have

$$\begin{aligned} \mathbb{E}\{\mathcal{L}V_1(x(t))\} &= 2x^{\mathrm{T}}(t)P\phi(t) \\ \mathbb{E}\{\mathcal{L}V_2(x(t))\} &= x^{\mathrm{T}}(t)(Q_1+Q_2+Q_3)x(t) - x^{\mathrm{T}}(t-\tau_m)Q_1x(t-\tau_m) - x^{\mathrm{T}}(t-\tau_0)Q_2x(t-\tau_0) \\ &\quad - x^{\mathrm{T}}(t-\tau_M)Q_3x(t-\tau_M) \\ \mathbb{E}\{\mathcal{L}V_3(x(t))\} &= \dot{x}^{\mathrm{T}}(t)(\tau_m^2 + \delta R_2 + \delta R_3)\dot{x}(t) - \tau_m\int_{t-\tau_m}^{t} \dot{x}^{\mathrm{T}}(s)R_1\dot{x}(s)\mathrm{d}s - \int_{t-\tau_0}^{t-\tau_m} \dot{x}^{\mathrm{T}}(s)R_2\dot{x}(s)\mathrm{d}s \\ &\quad - \int_{t-\tau_M}^{t-\tau_0} \dot{x}^{\mathrm{T}}(s)R_3\dot{x}(s)\mathrm{d}s \end{aligned} \tag{18}$$

Using Lemma 1, we have

$$-\tau_m \int_{t-\tau_m}^{t} \dot{x}^{\mathrm{T}}(s) R \dot{x}(s) \mathrm{d}s \leq \begin{bmatrix} x(t) \\ x(t-\tau_m) \end{bmatrix}^{\mathrm{T}} \begin{bmatrix} -R_1 & R_1 \\ R_1 & -R_1 \end{bmatrix} \begin{bmatrix} x(t) \\ x(t-\tau_m) \end{bmatrix} \tag{19}$$

Now we will discuss the derivation of $\mathbb{E}\{V(x(t))\}$ on sets Θ_1 and Θ_2, respectively.
Case 1: $t \in \Theta_1$, i.e., $\tau_m \leq \tau(t) \leq \tau_0$.
Similar to (19), we have

$$-\int_{t-\tau_M}^{t-\tau_0} \dot{x}^{\mathrm{T}}(s) R_3 \dot{x}(s) \mathrm{d}s \leq \begin{bmatrix} x(t-\tau_0) \\ x(t-\tau_M) \end{bmatrix}^{\mathrm{T}} \begin{bmatrix} -\frac{R_3}{\delta} & \frac{R_3}{\delta} \\ \frac{R_3}{\delta} & -\frac{R_3}{\delta} \end{bmatrix} \begin{bmatrix} x(t-\tau_0) \\ x(t-\tau_M) \end{bmatrix} \tag{20}$$

Combining (19) and (20) and with free weighting matrix technology, we have

$$\begin{aligned} \mathbb{E}\{\mathcal{L}V_3(x(t))\} &= \phi^{\mathrm{T}}(t)(\tau_m^2 R_1 + \delta R_2 + \delta R_3)\phi(t) + \alpha_0(1-\alpha_0)\psi^{\mathrm{T}}(t)(\tau_m^2 R_1 + \delta R_2 + \delta R_3)\psi(t) \\ &+ \begin{bmatrix} x(t) \\ x(t-\tau_m) \end{bmatrix}^{\mathrm{T}} \begin{bmatrix} -R_1 & R_1 \\ R_1 & -R_1 \end{bmatrix} \begin{bmatrix} x(t) \\ x(t-\tau_m) \end{bmatrix} \\ &+ \begin{bmatrix} x(t-\tau_0) \\ x(t-\tau_M) \end{bmatrix}^{\mathrm{T}} \begin{bmatrix} -\frac{R_3}{\delta} & \frac{R_3}{\delta} \\ \frac{R_3}{\delta} & -\frac{R_3}{\delta} \end{bmatrix} \begin{bmatrix} x(t-\tau_0) \\ x(t-\tau_M) \end{bmatrix} + \int_{t-\tau_0}^{t-\tau_m} \dot{x}^{\mathrm{T}}(s) R_2 \dot{x}(s) \mathrm{d}s \\ &+ 2\zeta^{\mathrm{T}}(t) N \big[x(t-\tau_m) - x(t-\tau(t)) - \int_{t-\tau(t)}^{t-\tau_m} \dot{x}(s) \mathrm{d}s \big] \\ &+ 2\zeta^{\mathrm{T}}(t) N \big[x(t-\tau(t)) - x(t-\tau_0) - \int_{t-\tau 0}^{t-\tau(t)} \dot{x}(s) \mathrm{d}s \big] \end{aligned}$$

where $\zeta = [x^{\mathrm{T}}(t), x^{\mathrm{T}}(t-\tau(t)), x^{\mathrm{T}}(t-\tau_m), x^{\mathrm{T}}(t-\tau_0), x^{\mathrm{T}}(t-\tau_M), w^{\mathrm{T}}(t), \xi^{\mathrm{T}}(t)]^{\mathrm{T}}$.
Then by Lemma 2, we can derive

$$\begin{aligned} -2\zeta^{\mathrm{T}}(t) N \int_{t-\tau(t)}^{t-\tau_m} \dot{x}(s) \mathrm{d}s &\leq (\tau(t)-\tau_m)\zeta^{\mathrm{T}}(t) N R_2^{-1} N^{\mathrm{T}} \zeta(t) + \int_{t-\tau(t)}^{t-\tau_m} \dot{x}^{\mathrm{T}}(s) R_2 \dot{x}(s) \mathrm{d}s \\ -2\zeta^{\mathrm{T}}(t) M \int_{t-\tau_0}^{t-\tau(t)} \dot{x}(s) \mathrm{d}s &\leq (\tau_0-\tau(t))\zeta^{\mathrm{T}}(t) N R_2^{-1} N^{\mathrm{T}} \zeta(t) + \int_{t-\tau_0}^{t-\tau(t)} \dot{x}^{\mathrm{T}}(s) R_2 \dot{x}(s) \mathrm{d}s \end{aligned} \tag{21}$$

With above analyses, we have

$$\begin{aligned} &\mathbb{E}\{\mathcal{L}V(x(t))\} + \mathbb{E}\{y^{\mathrm{T}}(t)y(t)\} - \gamma\mathbb{E}\{w^{\mathrm{T}}(t)w(t) + \xi^{\mathrm{T}}(t)\xi(t)\} \\ &= \zeta^{\mathrm{T}}(t)\Phi_1\zeta(t) + \zeta^{\mathrm{T}}(t)\mathcal{A}_\phi^{\mathrm{T}}(\tau_m^2 R_1 + \delta R_2 + \delta R_3)\mathcal{A}_\phi\zeta(t) \\ &+ \zeta^{\mathrm{T}}(t)\mathcal{A}_\psi^{\mathrm{T}}[\alpha_0(1-\alpha_0)(\tau_m^2 R_1 + \delta R_2 + \delta R_3)]A_\psi\zeta(t) \\ &+ \zeta^{\mathrm{T}}(t)(\Sigma_{11}^1 + \Sigma_{11}^{1\,\mathrm{T}})\zeta(t) + (\tau(t)-\tau_m)\zeta^{\mathrm{T}}(t)NR_2^{-1}N^{\mathrm{T}}\zeta(t) + (\tau_0-\tau(t))\zeta^{\mathrm{T}}(t)MR_2^{-1}M^{\mathrm{T}}\zeta(t) \end{aligned} \tag{22}$$

From (16) with $i = 1$, $j = 1, 2$, and according to Lemma 3 as well as Schur complement, one can derive

$$\mathbb{E}\{\mathcal{L}V(x(t))\} + \mathbb{E}\{y^{\mathrm{T}}(t)y(t)\} - \gamma\mathbb{E}\{w^{\mathrm{T}}(t)w(t) + \xi^{\mathrm{T}}(t)\xi(t)\} \leq 0 \tag{23}$$

Case 2: $t \in \Theta_2$, i.e., $\tau_0 \leq \tau(t) \leq \tau_M$.
By Lemma 1, we have

$$-\int_{t-\tau_0}^{t-\tau_m} \dot{x}^{\mathrm{T}}(s) R_3 \dot{x}(s) \mathrm{d}s \leq \begin{bmatrix} x(t-\tau_m) \\ x(t-\tau_0) \end{bmatrix}^{\mathrm{T}} \begin{bmatrix} -\frac{R_2}{\delta} & \frac{R_2}{\delta} \\ \frac{R_2}{\delta} & -\frac{R_2}{\delta} \end{bmatrix} \begin{bmatrix} x(t-\tau_m) \\ x(t-\tau_0) \end{bmatrix} \tag{24}$$

Then with

$$\begin{aligned}\zeta^{\mathrm{T}}(t)S\big[x(t-\tau_0)-x(t-\tau(t))-\int_{t-\tau(t)}^{t-\tau_0}\dot{x}(s)\mathrm{d}s\big]=0\\ \zeta^{\mathrm{T}}(t)T\big[x(t-\tau(t))-x(t-\tau_M)-\int_{t-\tau_M}^{t-\tau(t)}\dot{x}(s)\mathrm{d}s\big]=0\end{aligned} \tag{25}$$

and using similar methods in Case 1, we have

$$\begin{aligned}&\mathbb{E}\{\mathcal{L}V(x(t))\}+\mathbb{E}\{y^{\mathrm{T}}(t)y(t)\}-\gamma\mathbb{E}\{w^{\mathrm{T}}(t)w(t)+\xi^{\mathrm{T}}(t)\xi(t)\}\\ &=\zeta^{\mathrm{T}}(t)\Phi_2\zeta(t)+\zeta^{\mathrm{T}}(t)\mathcal{A}_\phi^{\mathrm{T}}(\tau_m^2R_1+\delta R_2+\delta R_3)\mathcal{A}_\phi\zeta(t)\\ &+\zeta^{\mathrm{T}}(t)\mathcal{A}_\psi^{\mathrm{T}}[\alpha_0(1-\alpha_0)(\tau_m^2R_1+\delta R_2+\delta R_3)]A_\psi\zeta(t)\\ &+\zeta^{\mathrm{T}}(t)(\Sigma_{11}^2+\Sigma_{11}^{2\ \mathrm{T}})\zeta(t)+(\tau(t)-\tau_m)\zeta^{\mathrm{T}}(t)SR_2^{-1}S^{\mathrm{T}}\zeta(t)+(\tau_0-\tau(t))\zeta^{\mathrm{T}}(t)TR_2^{-1}T^{\mathrm{T}}\zeta(t)\end{aligned} \tag{26}$$

which also leads to (23) according to (16) with $i=1$ and $j=1,2$. Thus combining the results of two cases above, we have

$$\mathbb{E}\{\mathcal{L}V(x(t))\}\le-\mathbb{E}\{y^{\mathrm{T}}(t)y(t)\}+\gamma\mathbb{E}\{w^{\mathrm{T}}(t)w(t)+\xi^{\mathrm{T}}(t)\xi(t)\} \tag{27}$$

If $w(t)=0$ and $\xi(t)=0$, one can easily have $\mathbb{E}\{\mathcal{L}V(x(t))\}\le 0$, which implies system (15) with $w(t)=0$ and $\xi(t)=0$ is asymptotically stable. With the presence of disturbance input and deception attack, integrating both sides of (27) from t_0 to t with $t\to+\infty$, we can have $\mathbb{E}\{y^{\mathrm{T}}(t)y(t)\}\le\gamma\mathbb{E}\{w^{\mathrm{T}}(t)w(t)+\xi^{\mathrm{T}}(t)\xi(t)$, which completes the proof. □

Remark 2. *A piecewise delay analysis method is adopted in constructing Lyapunov–Krasovskii functional candidate. Specifically, the time delay variation interval is divided into two subintervals with equal length, which can effectively reduce the conservativeness of the results. Furthermore, the delay interval can also be divided into more than two subsets, which can lead to less conservativeness [18].*

3.2. Networked Load Frequency Controller Design

As we can see, when controller gain K is unknown, the inequality in Theorem 1 is nonlinear, which cannot be solved directly. In this subsection, we are going to present the design approach to gain K based on Theorem 1.

Theorem 2. *For given scalars $\alpha_0\ge 0$, $\gamma>0$, $\tau_M\ge\tau_m\ge 0$, system (12) is asymptotically stable satisfying H_∞ performance if there exist positive definite matrices X, Y, $\tilde{R}_1$, $\tilde{R}_2$, $\tilde{R}_3$, $\tilde{M}$, $\tilde{N}$, $\tilde{S}$ and $\tilde{T}$ such that the following inequalities hold:*

$$\begin{bmatrix}\tilde{\Phi}_i+\tilde{\Sigma}_{11}^i+(\tilde{\Sigma}_{11}^i)^{\mathrm{T}} & * & * & \\ \tilde{\Sigma}_{21}^{ij} & \tilde{\Sigma}_{22}^i & * & \\ \tilde{\Sigma}_{31} & 0 & \tilde{\Sigma}_{33} & \\ \tilde{\Sigma}_{41} & 0 & 0 & -I\end{bmatrix}<0,\ i=1,2\ j=1,2 \tag{28}$$

where

$$\tilde{\Phi}_1=\begin{bmatrix}\tilde{\Phi}_{11} & * & * & * & * & * & *\\ (1-\alpha_0)Y^{\mathrm{T}}B^{\mathrm{T}} & 0 & * & * & * & * & *\\ \tilde{R}_1 & 0 & -\tilde{Q}_1-\tilde{R}_1 & * & * & * & *\\ 0 & 0 & 0 & -\tilde{Q}_2-\frac{\tilde{R}_3}{\delta} & * & * & *\\ 0 & 0 & 0 & \frac{\tilde{R}_3}{\delta} & -\tilde{Q}_3-\frac{\tilde{R}_3}{\delta} & * & *\\ F^{\mathrm{T}} & 0 & 0 & 0 & 0 & -\gamma^2I & *\\ \alpha_0B^{\mathrm{T}}X & 0 & 0 & 0 & 0 & 0 & -\gamma^2I\end{bmatrix}$$

$$\tilde{\Phi}_1^{11} = AX + XA^{\mathrm{T}} + \tilde{Q}_1 + \tilde{Q}_2 + \tilde{Q}_3 - \tilde{R}_1$$

$$\tilde{\Phi}_2 = \begin{bmatrix} \tilde{\Phi}_{11} & * & * & * & * & * & * \\ (1-\alpha_0)Y^{\mathrm{T}}B^{\mathrm{T}} & 0 & * & * & * & * & * \\ \tilde{R}_1 & 0 & -\tilde{Q}_1 - \tilde{R}_1 - \frac{\tilde{R}_2}{\delta} & * & * & * & * \\ 0 & 0 & \frac{\tilde{R}_2}{\delta} & -\tilde{Q}_2 - \frac{\tilde{R}_2}{\delta} & * & * & * \\ 0 & 0 & 0 & 0 & -\tilde{Q}_3 & * & * \\ F^{\mathrm{T}} & 0 & 0 & 0 & 0 & -\gamma^2 I & * \\ \alpha_0 B^{\mathrm{T}} X & 0 & 0 & 0 & 0 & 0 & -\gamma^2 I \end{bmatrix}$$

$$\tilde{\Sigma}_{11}^1 = \begin{bmatrix} 0 & -\tilde{N} + \tilde{M} & \tilde{N} & -\tilde{M} & 0 & 0 & 0 \end{bmatrix}$$

$$\tilde{\Sigma}_{11}^2 = \begin{bmatrix} 0 & \tilde{T} - \tilde{S} & 0 & \tilde{S} & -\tilde{T} & 0 & 0 \end{bmatrix}$$

$$\tilde{\Sigma}_{21}^{11} = \sqrt{\delta}\tilde{N}^{\mathrm{T}},\ \tilde{\Sigma}_{21}^{12} = \sqrt{\delta}\tilde{M}^{\mathrm{T}},\ \tilde{\Sigma}_{21}^{21} = \sqrt{\delta}\tilde{S}^{\mathrm{T}},\ \tilde{\Sigma}_{21}^{22} = \sqrt{\delta}\tilde{T}^{\mathrm{T}}$$

$$\tilde{\Sigma}_{22}^1 = -\tilde{R}_2,\ \Sigma_{22}^2 = -\tilde{R}_3$$

$$\tilde{\Sigma}_{31} = \begin{bmatrix} \tau_m \tilde{R}_1 \tilde{\mathcal{A}}_\phi \\ \sqrt{\delta}\tilde{R}_2 \tilde{\mathcal{A}}_\phi \\ \sqrt{\delta}\tilde{R}_3 \tilde{\mathcal{A}}_\phi \\ \tau_m \sqrt{\alpha_0(1-\alpha_0)\delta}\tilde{R}_1 \tilde{\mathcal{A}}_\psi \\ \sqrt{\alpha_0(1-\alpha_0)\delta}\tilde{R}_2 \tilde{\mathcal{A}}_\psi \\ \sqrt{\alpha_0(1-\alpha_0)\delta}\tilde{R}_3 \tilde{\mathcal{A}}_\psi \end{bmatrix},\ \tilde{\Sigma}_{33} = \mathrm{diag}\{-\tilde{R}_1, -\tilde{R}_2, -\tilde{R}_3, -\tilde{R}_1, -\tilde{R}_2, -\tilde{R}_3\}$$

$$\tilde{\mathcal{A}}_\phi = \begin{bmatrix} AX & BY & 0 & 0 & 0 & FX & \alpha_0 BX \end{bmatrix}$$

$$\tilde{\mathcal{A}}_\psi = \begin{bmatrix} 0 & BY & 0 & 0 & 0 & 0 & -BX \end{bmatrix}$$

Proof of Theorem 2. Let $X = P^{-1}$, $\tilde{R}_i = XR_iX$, $Y = KCX$, $\tilde{Q}_i = XQ_iX$, $i = 1,2,3$, $\tilde{M} = XMX$, $\tilde{N} = XNX$, $\tilde{S} = XSX$, $\tilde{T} = XTX$. Then pre- and post-multiplying inequality (16) with $\mathrm{diag}\{X, X, X, X, X, I, I, X, R_1^{-1}, R_2^{-1}, R_3^{-1}, R_1^{-1}, R_2^{-1}, R_3^{-1}\}$, and together with Schur complement, one can easily arrive at inequality (28). □

In the case where K is unknown, linear matrix inequality (28) provided in Theorem 2 is solvable. However, the controller gain is still unsolvable due to the nonlinearity form KCX. Now we are in the position to design controller gain. In the following, we use a similar method in [23] for linearization.

Theorem 3. *For given scalars $\alpha_0 \geq 0$, $\gamma > 0$, $\tau_M \geq \tau_m \geq 0$, system (12) is asymptotically stable satisfying H_∞ performance if there exist positive definite matrices X, Y $\tilde{R}_1$, $\tilde{R}_2$, $\tilde{R}_3$, $\tilde{M}$, $\tilde{N}$, $\tilde{S}$ and $\tilde{T}$ such that the following inequalities hold:*

$$\begin{bmatrix} \tilde{\Phi}_i' + \tilde{\Sigma}_{11}^{i'} + (\tilde{\Sigma}_{11}^{i'})^{\mathrm{T}} & * & * \\ \tilde{\Sigma}_{21}^{ij'} & \tilde{\Sigma}_{22}^{i'} & * \\ \tilde{\Sigma}_{31}' & 0 & \tilde{\Sigma}_{33}' \\ \tilde{\Sigma}_{41}' & 0 & 0 \end{bmatrix} \begin{matrix} \\ \\ \\ -I \end{bmatrix} < 0,\ i = 1,2\ j = 1,2 \tag{29}$$

$$\begin{bmatrix} -\epsilon I & * \\ VC - CX & -I \end{bmatrix} < 0,\ \epsilon \to 0 \tag{30}$$

where $\tilde{\Phi}_i'$, $\tilde{\Sigma}_{11}^{i'}$, $\tilde{\Sigma}_{21}^{ij'}$, $\tilde{\Sigma}_{22}^{i'}$, and $\tilde{\Sigma}_{41}'$ can be obtained from $\tilde{\Phi}_i$, $\tilde{\Sigma}_{11}^{i}$, $\tilde{\Sigma}_{21}^{ij}$, $\tilde{\Sigma}_{22}^{i}$, and $\tilde{\Sigma}_{41}$ by replacing KCX with UC, respectively. Sequently, the load frequency controller gain can be computed with $K = UV^{-1}$.

Proof of Theorem 3. To solve the infeasible term KCX, we let $VC = CX$. The coupling terms KCX in inequality (28) would be transformed into a W-problem proposed in [30]. Then using an alternative method in [27], we have $(VC - CX)^{\mathrm{T}}(VC - CX) = 0$, which leads to optimization problem (30) according to schur complement. Since C is full row rank matrix, one can deduce that M is full rank and invertible. Thus together with $KCX = UC$, the output feedback gain can be calculated by $K = UV^{-1}$. □

With the design approach proposed in Theorem 3, PI controller gains for multiple power systems can be computed through solving the linear matrix inequalities (29) and (30) using YALMIP toolbox with SeDuMi optimization in MATLAB (R2016a).

4. A Case Study

In this section, we are going to present a practical network-based load frequency control for multi-area power systems in smart grid. In the numerical simulation, an interconnected three-area smart grid is considered. The parameters of three areas are chosen as follows [31].

Area 1: $D_1 = 1$, $M_1 = 10$, $R_1 = 0.05$, $T_{ch1} = 0.3s$, $T_{g1} = 0.1s$, $\beta_1 = \frac{2}{R_1} + D_1$.
Area 2: $D_2 = 1.5$, $M_2 = 12$, $R_2 = 0.05$, $T_{ch2} = 0.17s$, $T_{g2} = 0.4s$, $\beta_2 = \frac{4}{R_2} + D_2$.
Area 3: $D_3 = 1.8$, $M_3 = 12$, $R_3 = 0.05$, $T_{ch3} = 0.02s$, $T_{g3} = 0.35s$, $\beta_3 = \frac{3}{R_3} + D_3$.

In addition, we set $T_{12} = 0.2p.u./rad$, $T_{23} = 0.12p.u./rad$, $T_{31} = 0.25p.u./rad$, $\alpha_0 = 0.3$, and the sampling period $h = 0.01s$. The deception attack signal is chosen as $\xi(t) = [0.1\exp^{-0.01t}\sin(0.1t), 0.05\exp^{-0.01t}\sin(0.12t), 0.15\exp^{-0.01t}\sin(0.1t)]^{\mathrm{T}}$. In the following we are going to present an algorithm to implement the output feedback PI controller design.

By using Algorithm 1, we can design the network-based load frequency control scheme for multiple area power systems with communication under deception attacks. Specifically, matrices U, V and K can be calculated as follows.

$$U = \begin{bmatrix} -0.1315 & -0.1392 & -0.0580 & 0.1356 & -0.0310 & -0.0160 \\ 0.0873 & -0.1089 & -0.0445 & -0.0047 & 0.0589 & -0.2566 \\ 0.1119 & 0.1158 & -0.0116 & -0.2923 & -0.0806 & -0.2823 \end{bmatrix},$$

$$V = \begin{bmatrix} 0.9213 & -0.1039 & 0.3873 & -0.5374 & 0.0218 & 1.0320 \\ 0.0284 & 1.0932 & 0.0312 & -0.4359 & 0.1994 & -0.9024 \\ 0.1435 & 0.2947 & 0.2498 & 0.0002 & 0.0982 & 0.9175 \\ -1.2934 & 0.4358 & -0.1434 & 0.0494 & -0.8763 & 0.4711 \\ 0.1044 & 0.0014 & 0.0003 & 0.8624 & 0.9724 & 0.8163 \\ -1.0693 & -0.9324 & 0.0927 & 0.9427 & -0.9375 & 0.9375 \end{bmatrix}$$

$$K = \begin{bmatrix} -0.1384 & -0.1405 & 0.0000 & 0.0000 & 0.0000 & 0.0000 \\ 0.0000 & 0.0000 & -0.2318 & -0.0932 & 0.0000 & 0.0000 \\ 0.0000 & 0.0000 & 0.0000 & 0.0000 & -0.2029 & -0.1245 \end{bmatrix},$$

which implies the controller gains of corresponding three areas are $K_1 = [-0.1384, -0.1405]$, $K_2 = [-0.2318, -0.0932]$, $K_3 = [-0.2029, -0.1245]$. As is seen, without a secure control mechanism, the deviation of frequency of three-area power systems encountered in deception attacks is shown in Figure 2, which cannot reach stable performance. In the sequent, the evolution of frequency deviation of the attacked three-area power systems with secure control scheme is given in Figure 3, which shows the effectiveness of the designed control strategy. Furthermore, we can see that deception attacks were launched 593 times into the communication network. The evolution of stochastic variable $\alpha(t)$ in the first five seconds is given in Figure 4, where $\alpha(t) = 1$ implies the deception attack is launched into network at time t. Besides, the deceptive signal $\alpha(t)v(t)$ launched into the communication network is shown in Figure 5, from which one can clearly see the attack instants and the corresponding values of a deceptive signal.

Algorithm 1 Output feedback PI load frequency controller design for three-area power systems.

Require: D_i, M_i, R_i, T_{chi}, T_{gi}, β_i, T_{ij}, $i = 1,2,3$, $j = 1,2,3$, α_0.

Ensure: The given parameters are reasonable in describing multi-area power systems with Equations (1)–(6);

1: Using the input parameters to calculate the corresponding matrices in the augmented system (7) including A_{ii}, A_{ij}, B_i, F_i, C_i, $i = 1,2,3$, $j = 1,2,3$;
2: Solving linear matrix inequalities (29) and (30) using YALMIP toolbox with SeDuMi optimization;
3: Gaining matrices U, V;
4: Calculating $K = UV^{-1}$; **return** K;

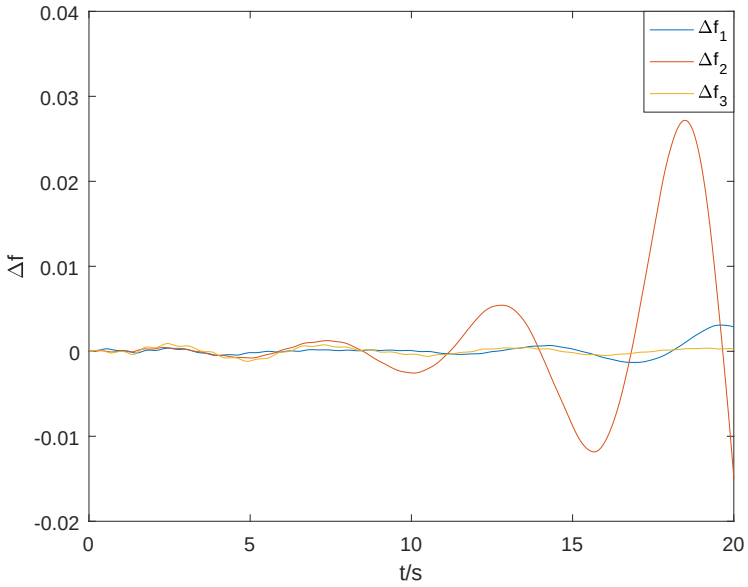

Figure 2. Frequency deviation of three areas without secure control scheme.

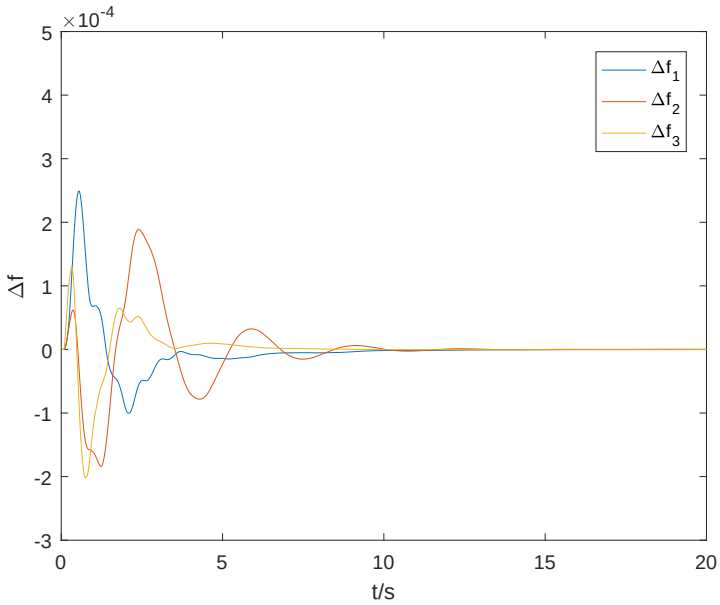

Figure 3. Frequency deviation of three areas with secure control scheme.

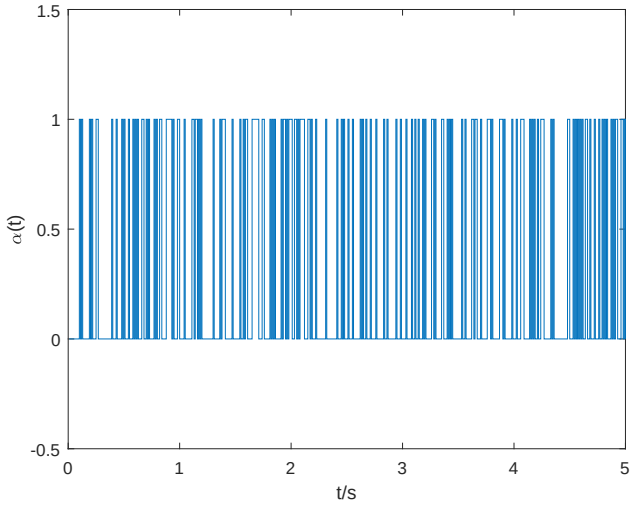

Figure 4. The evolution of $\alpha(t)$.

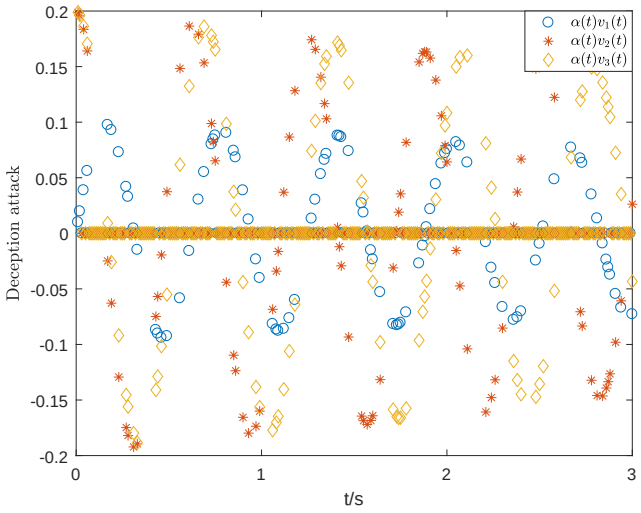

Figure 5. Deception attack $\alpha(t)v(t)$.

5. Conclusions

The network-based Load frequency control problem of multiple area power systems against deception attacks has been investigated in this paper. With data transmitted through a wireless network, packets may be delayed or dropped in communication channels, and may also be corrupted by stochastic deception attacks. A dedicated system model has been provided to account for these negative effects on system performance. Based on the established model, the LFC problem has been investigated with a piecewise delay analysis method which is of less conservativeness. A controller design approach has been proposed in terms of linear matrix inequalities. A numerical example of three area power systems has been given to demonstrate the obtained results.

Author Contributions: Conceptualization, J.Y. and F.Z.; methodology, F.Z.; software, N.W.; validation, J.Y. and F.Z.; formal analysis, F.Z.; investigation, F.Z. and H.W.; resources, J.Y. and Z.Z.; data curation, N.W. and Z.Z.; writing—original draft preparation, F.Z.; writing—review and editing, J.Y. and F.Z.; supervision, N.W. and H.W.; project administration, N.W. and F.Z.; funding acquisition, F.Z. and Z.Z.

Funding: This research was funded by the Fundamental Research Funds for the Central Universities (2015MS83).

Conflicts of Interest: The authors declare no conflict of interest.

References

1. Singh, V.P.; Kishor, N.; Samuel, P. Distributed multi-agent system-based load frequency control for multi-area power system in smart grid. *IEEE Trans. Ind. Electron.* **2017**, *64*, 5151–5160. [CrossRef]
2. Elgerd, O.; Fosha, C. The research for multi-area frequency control problem. *IEEE Trans. PAS Power Appar Syst.* **1970**, *89*, 551–556.
3. Talaq, J.; Al-Basri, F. Adaptive fuzzy gain scheduling for load frequency control. *IEEE Trans. Power Syst.* **1999**, *14*, 145–150. [CrossRef]
4. Rerkpreedapong, D.; Hasanovic, A.; Feliachi, A. Robust load frequency control using genetic algorithms and linear matrix inequalities. *IEEE Trans. Power Syst.* **2003**, *18*, 855–861. [CrossRef]
5. Yang, J.; Zeng, Z.; Tang, Y.; Yan, J.; He, H.; Wu, Y. Load frequency control in isolated micro-grids with electrical vehicles based on multivariable generalized predictive theory. *Energies* **2015**, *8*, 2145–2164. [CrossRef]
6. Liao, K.; Xu, Y. A robust load frequency control scheme for power systems based on second-order sliding mode and extended disturbance observer. *IEEE Trans. Ind. Inform.* **2018**, *14*, 3076–3086. [CrossRef]
7. Topno, P.N.; Chanana, S. Load frequency control of a two-area multi-source power system using a tilt integral derivative controller. *J. Vib. Control* **2018**, *24*, 110–125. [CrossRef]
8. Khooban, M.H.; Niknam, T.; Shasadeghi, M.; Dragicevic, T.; Blaabjerg, F. Load frequency control in microgrids based on a stochastic noninteger controller. *IEEE Trans. Sustain. Energy* **2018**, *9*, 853–861. [CrossRef]
9. Charles, K.; Urasaki, N.; Senjyu, T.; Elsayed Lotfy, M.; Liu, L. Robust load frequency control schemes in power system using optimized PID and model predictive controllers. *Energies* **2018**, *11*, 3070. [CrossRef]
10. Walsh, G.C.; Ye, H.; Bushnell, L.G. Stability analysis of networked control systems. *IEEE Trans. Control Syst. Technol.* **2002**, *10*, 438–446. [CrossRef]
11. Yue, D.; Han, Q.L.; Peng, C. State feedback controller design of networked control systems. In *Proceedings of the 2004 IEEE International Conference on Control Applications*; IEEE: Piscataway Township, NJ, USA, 2004; Volume 1, pp. 242–247.
12. Zhang, X.M.; Han, Q.L.; Yu, X. Survey on recent advances in networked control systems. *IEEE Trans. Ind. Inform.* **2016**, *12*, 1740–1752. [CrossRef]
13. Ge, X.; Yang, F.; Han, Q.L. Distributed networked control systems: A brief overview. *Inf. Sci.* **2017**, *380*, 117–131. [CrossRef]
14. Xiao, S.; Zhang, Y.; Zhang, B. Event-triggered network-based state observer design of positive systems. *Inf. Sci.* **2018**, *469*, 30–43. [CrossRef]
15. Zhang, H.; Shi, Y.; Wang, J.; Chen, H. A new delay-compensation scheme for networked control systems in controller area networks. *IEEE Trans. Ind. Electron.* **2018**, *65*, 7239–7247. [CrossRef]
16. He, Y.; Wu, M.; She, J.H.; Liu, G.P. Parameter-dependent Lyapunov functional for stability of time-delay systems with polytopic-type uncertainties. *IEEE Trans. Autom. Control* **2004**, *49*, 828–832. [CrossRef]
17. Shustin, E.; Fridman, E. On delay-derivative-dependent stability of systems with fast-varying delays. *Automatica* **2007**, *43*, 1649–1655. [CrossRef]
18. Yue, D.; Tian, E.; Zhang, Y. A piecewise analysis method to stability analysis of linear continuous/discrete systems with time-varying delay. *Int. J. Robust Nonlinear Control* **2009**, *19*, 1493–1518. [CrossRef]
19. Yue, D. Robust stabilization of uncertain systems with unknown input delay. *Automatica* **2004**, *40*, 331–336. [CrossRef]
20. Yuan, Y.; Li, Z.; Ren, K. Modeling load redistribution attacks in power systems. *IEEE Trans. Smart Grid* **2011**, *2*, 382–390. [CrossRef]
21. Liu, X.; Li, Z. Local load redistribution attacks in power systems with incomplete network information. *IEEE Trans. Smart Grid* **2014**, *5*, 1665–1676. [CrossRef]
22. Sargolzaei, A.; Yen, K.K.; Abdelghani, M.N. Preventing time-delay switch attack on load frequency control in distributed power systems. *IEEE Trans. Smart Grid* **2016**, *7*, 1176–1185. [CrossRef]
23. Peng, C.; Li, J.; Fei, M. Resilient Event-Triggering H_∞ Load Frequency Control for Multi-Area Power Systems With Energy-Limited DoS Attacks. *IEEE Trans. Power Syst.* **2017**, *32*, 4110–4118. [CrossRef]
24. Wu, Y.; Wei, Z.; Weng, J.; Li, X.; Deng, R.H. Resonance attacks on load frequency control of smart grids. *IEEE Trans. Smart Grid* **2018**, *9*, 4490–4502. [CrossRef]

25. Dagoumas, A. Assessing the Impact of Cybersecurity Attacks on Power Systems. *Energies* **2019**, *12*, 725. [CrossRef]
26. Xiao, S.; Han, Q.L.; Ge, X.; Zhang, Y. Secure distributed finite-time filtering for positive systems over sensor networks under deception attacks. *IEEE Trans. Cybern.* **2019**, 1–10. [CrossRef]
27. Peng, C.; Zhang, J. Delay-distribution-dependent load frequency control of power systems with probabilistic interval delays. *IEEE Trans. Power Syst.* **2015**, *31*, 3309–3317. [CrossRef]
28. Han, Q.L. Absolute stability of time-delay systems with sector-bounded nonlinearity. *Automatica* **2005**, *41*, 2171–2176. [CrossRef]
29. Sanchez, E.N.; Perez, J.P. Input-to-state stability (ISS) analysis for dynamic neural networks. *IEEE Trans. Circuits Syst. I Fundam. Theory Appl.* **1999**, *46*, 1395–1398. [CrossRef]
30. Crusius, C.A.; Trofino, A. Sufficient LMI conditions for output feedback control problems. *IEEE Trans. Autom. Control* **1999**, *44*, 1053–1057. [CrossRef]
31. Wen, S.; Yu, X.; Zeng, Z.; Wang, J. Event-triggering load frequency control for multiarea power systems with communication delays. *IEEE Trans. Ind. Electron.* **2016**, *63*, 1308–1317. [CrossRef]

© 2019 by the authors. Licensee MDPI, Basel, Switzerland. This article is an open access article distributed under the terms and conditions of the Creative Commons Attribution (CC BY) license (http://creativecommons.org/licenses/by/4.0/).